

Title:

Electronic, Magnetic and Structural Properties of the $R\text{FeO}_3$ Antiferromagnetic-Perovskites at Very High Pressures

Author(s):

Moshe P. Pasternak, W. M. Xu, G. Kh. Rozenberg, and R. D. Taylor

Submitted to:

<http://lib-www.lanl.gov/cgi-bin/getfile?00937171.pdf>

Electronic, Magnetic and Structural Properties of the $R\text{FeO}_3$ Antiferromagnetic-Perovskites at Very High Pressures

Moshe P. Pasternak, W. M. Xu, G. Kh. Rozenberg, and R. D. Taylor¹

School of Physics and Astronomy, Tel Aviv University,
Tel Aviv, ISRAEL,

¹MST-10, Los Alamos National Laboratory,
Los Alamos, NM 87545, U.S.A.

ABSTRACT

At ambient pressure the orthorhombic perovskites R -orthoferrites ($R \equiv \text{Lu}, \text{Eu}, \text{Y}, \text{Pr},$ and La) exhibit very large optical gaps. These large-gap *Mott* insulators in which the $3d^5$ high-spin ferric ions carry large local moments and magnetically order at $T_N > 600$ K, undergo a sluggish structural first-order phase transition in the 30-50 GPa range, with the exception of the LuFeO_3 which undergoes an isostructural volume reduction resulting from a high to low-spin crossover. High-pressure methods to 170 GPa using Mössbauer spectroscopy, resistance, and synchrotron-based XRD in diamond anvil cells were applied. Following the quasi-isostructural volume reduction (3-5%) the new phase the magnetic-ordering temperature is drastically reduced, to ~ 100 K, the direct and super-exchange interactions are drastically weakened, and the charge-transfer gap is substantially reduced. The high-pressure (HP) phases of the La and Pr oxides, at their inception, are composed of *high*- and *low*-spin Fe^{3+} magnetic sublattices, the abundance of the latter increasing with pressure but HP phases of the $\text{Eu}, \text{Y},$ and Lu oxides consist solely of low-spin Fe^{3+} . Resistance and Mössbauer studies in La and Pr orthoferrites reveal the onset of a metallic state with moments starting at $P > 120$ GPa. Based on the magnetic and electrical data of the latter species, a *Mott* phase diagram was established.

INTRODUCTION

The *rare-earth* orthoferrites - $R\text{FeO}_3$ - crystallize in a distorted orthorhombic structure, a derivative of cubic perovskite, with space group $Pbnm$. The unit cell contains four equivalent Fe^{3+} ions situated at octahedral centers formed by six nearest-neighbor oxygens. The tilting of the octahedral axes with respect to the c -axis is minimal, of the order of 10 mrad.[1]. The common apex of two adjacent octahedral is the intervening R^{3+} cation that provides the superexchange interaction path between two iron atoms. Thus, each iron ion is coupled by superexchange to six iron nearest neighbors resulting in relatively high Néel temperatures (T_N) ranging from 620 to 740 K for Lu and La , respectively. The ferric ions are antiferromagnetically coupled. The main motivation for this systematic study is the unique opportunity to vary the R -cation size, keeping practically the same ambient-pressure crystallographic structure and same nature of the R^{3+} - O chemical bond thus allowing to examine the effect of the R^{3+} ionic radii, which range from 86 pm (Lu^{3+}) to 103.2 pm (La^{3+}), on the evolution and properties of the ensuing new high-pressure phases.

Recently a detailed experimental study of the pressure-induced *Mott-Hubbard* phase diagram of the *large* La - and Pr -orthoferrites has been published [2]. Those results and previously,

in hematite (Fe_2O_3) [3], are the only cases in which concurrent *structural* and *electronic* transition has been reported for transition-metal ions in the d^5 state such as ferric oxide. In this paper we report systematic studies of the high-pressure (HP) structural, magnetic, and electronic properties of the $R\text{FeO}_3$ perovskite series with representative rare-earth compositions within the large (La^{3+} , Pr^{3+}), the intermediate (Eu^{3+} , Y^{3+}), to the smallest, Lu^{3+} R -cations. These compounds, characterized by large optical gaps and large on-site Fe^{3+} magnetic moments determined by Hund's rules, may in principle undergo an insulator-metal transition either by filling of carriers due to chemical doping or by high external pressure [4]. Whereas the first process will affect the U/t ratio by decreasing the value of U [5], the aftermath of the second process will be an increase of the d -band width W and therefore of the kinetic energy t . In principle both methods can provide variations in U/t for the investigation of the *Mott-Hubbard* system phase diagram. However, the main problem with chemical doping is that intricate and uncontrollable interactions may occur in such narrow d -band systems resulting in an undesired electronic and structural disorder and other complex phenomena unrelated to the *Mott-Hubbard* phenomenon [6]. Thus, external static pressure is the cleanest, most preferable way to study the phase diagram of a *Mott-insulator* in terms of U/t only.

Studies were carried out using the combined methods of synchrotron X-ray diffraction (XRD), electrical resistance ($R(P,T)$), and ^{57}Fe Mössbauer Spectroscopy (MS) in conjunction with diamond anvil cells at static pressures to ~ 200 GPa.

EXPERIMENTAL DETAILS

The $R\text{FeO}_3$ were synthesized by a solid-solid reaction in air of stoichiometric amounts of spectroscopical pure $R_2\text{O}_3$ and Fe_2O_3 (enriched to 25% ^{57}Fe) at 1200°C . The composition and magnetic properties of the samples at ambient pressure were confirmed by conventional powder

Parameters	Configuration	LaFeO_3	PrFeO_3	EuFeO_3	YFeO_3	LuFeO_3
IS (mm/s)	LP	0.220(1)	0.240(1)	0.23(2)	0.24(2)	0.24(2)
	HP, $S=5/2$	0.063(2)	0.134(1)			
	HP, $S=1/2$	0.036(2)	0.09(2)	0.05(1)	0.14(1)	0.23(2)
QS (mm/s)	LP	0.37(4)	0.24(3)	0.12(2)	0.11(2)	0.00(2)
	HP, $S=5/2$	0.590(3)	0.550(2)			
	HP, $S=1/2$	1.193(2)	1.230(3)	0.550(3)	1.420(7)	1.384(5)
H_{hf} (T)	LP	51.6(2)	52.4(2)	52.7(2)	50.6(2)	50.6(2)
	HP, $S=5/2$	46.0(2)	47.2(2)			
	$S=1/2$	37.5(2)	35.3(2)	30.3(3)	26.4(2)	14.3(4)
T_N (K)	LP	740	707	662	640	623
T_M (K)	HP	105	100	90	70	50
P_c (GPa)		40	44	47	55	55

Table 1. Values of the hyperfine interaction parameters deduced from the least-squares fitting to the experimental Mössbauer spectra. The LP parameters are from spectra recorded at $P = P_c$. Numbers in parentheses are the statistical error, IS values are with respect to $\alpha\text{-Fe}$ at RT, LP quadrupole splitting (QS) values were deduced from the shift of the Zeeman splitting, and T_N values were adopted from Ref. 1, T_M is the magnetic-ordering temperature of the HP species,

XRD and MS. The *Tel-Aviv University* (TAU) miniature piston/cylinder DAC [7] was used with anvils having $\sim 200\text{-}\mu\text{m}$ diameter culet size. Samples were encapsulated in $100\text{-}\mu\text{m}$ cavities drilled in stainless-steel gaskets for XRD and resistance measurements and in a Re gasket for MS studies. Re also served as a collimator for the 14.4-keV γ -rays. For the XRD and MS studies Ar was used as a pressurizing medium [8]. Ruby fluorescence served as a manometer.

X-ray diffraction measurements with synchrotron radiation were carried out at 300 K in the angle dispersive mode using the monochromatic beam of the ID30 station at the *European Synchrotron Radiation Facilities* (ESRF) and the diffraction images were collected at $\lambda = 0.4246 \text{ \AA}$ wavelength using image plates with typical exposure times of 5 minutes. Data were analyzed using the FIT2D program [9].

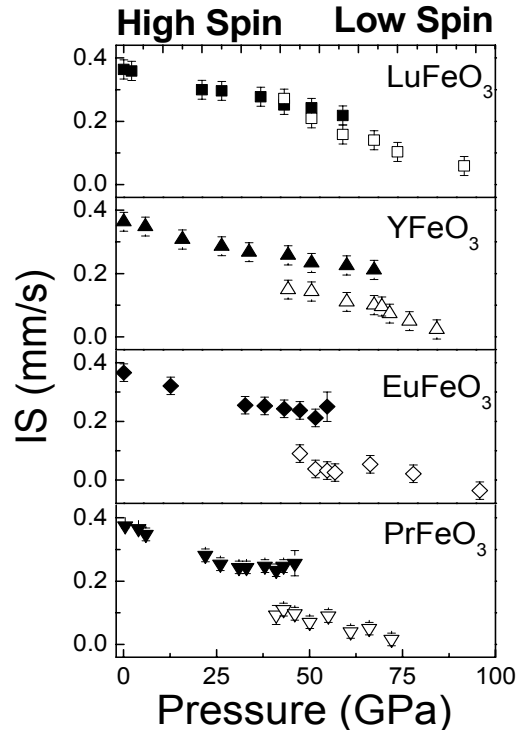


Figure 1. Pressure dependence of the IS for the various orthoferrites. The open symbols correspond to the LS states.

Resistance studies in the 4 – 300 K range were performed with miniature Pt electrodes insulated from the metal gasket by a mixture of alumina and NaCl. The DAC was mounted in a special holder device inserted into a commercial LHe Dewar. Using a PC-controlled DC motor-drive system, the DAC was gradually lowered and cooled by the cold He gas while recording simultaneously the temperature from a calibrated Si-diode thermometer and the resistance using the four-probe method.

Mössbauer studies were carried out with a $^{57}\text{Co(Rh)}$ 10-mCi point source in the 4 – 300 K temperature range using a top-loading LHe cryostat [10]. Typical collection time of a single spectrum was ~ 24 hours. All spectra were analyzed using appropriate fitting programs from which the hyperfine interaction parameters and the corresponding relative abundances of spectral components were derived.

RESULTS

The hyperfine interaction parameters deduced from the least-squares fitting of the experimental Mössbauer spectra are given in table I. The parameters for the low-pressure (LP) phase were obtained for the highest pressure prior to the phase transition.

The smallest orthoferrite; LuFeO₃

Mössbauer spectra of LuFeO₃ at 300 K recorded at several pressures are shown in Fig. 2a. It is evident that between 25 – 42 GPa a sluggish magnetic/electronic phase transition occurs and is concluded at ~ 70 GPa. The magnetic to non-magnetic transition signals either a *Mott* transition, in which an insulator-metal transition takes place, or an ordered to a disordered magnetic transition resulting in a paramagnetic state. Preliminary analysis of our XRD data points to a unremitting presence of an orthorhombic structure with a volume drop at P_C of ~5%. Note (see Fig. 1) that within the experimental methods there is no drop in the IS [11] at P_C .

By cooling the sample at 70 GPa to cryogenic temperatures one clearly observes the onset of a magnetic ordering at $T_M \sim 50$ K (see Fig. 2b). This magnetic ordering is mediated by a *weak* spin-spin interaction resulting in spin-spin ($S = -1/2 \leftrightarrow S = +1/2$) relaxation Mössbauer spectra [2]

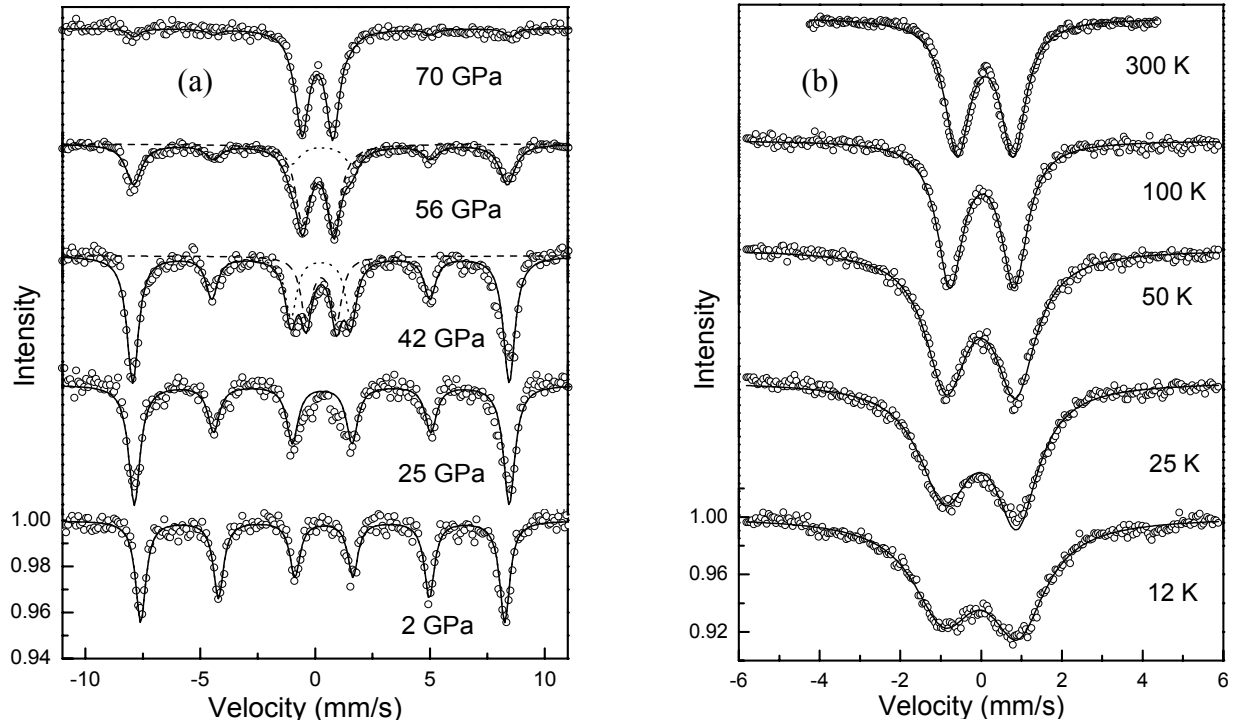


Figure 2. (a) The evolution of the HP phase in LuFeO₃ as observed by MS at RT. The HP phase is paramagnetic and characterized by a single quadrupole-split component. (b) The onset of the magnetic ordering of the LS ferric moments at $T < 50$ K. Solid lines are the convoluted theoretical fit to the experimental spectra. The dotted lines correspond to the spectral components.

in which the Zeeman hyperfine manifold fluctuates within a characteristic fluctuating time τ , of the order of the 14.4 keV nuclear lifetime $\tau_{1/2}$ ($\sim 10^{-7}$ s). This is a consequence of spin crossover, an electronic transition from a *high* to a low *spin* (${}^6A_{1g} \rightarrow {}^2T_{2g}$) due to the substantial increase of the crystal field as a result of pressure [12].

Despite the continuous albeit significant drop in the resistance, The Lu-orthoferrite remains an insulator up to 80 GPa. The R(P) curve is shown in Fig 3 and the R(T) curves for the highest pressures are shown on the inset.

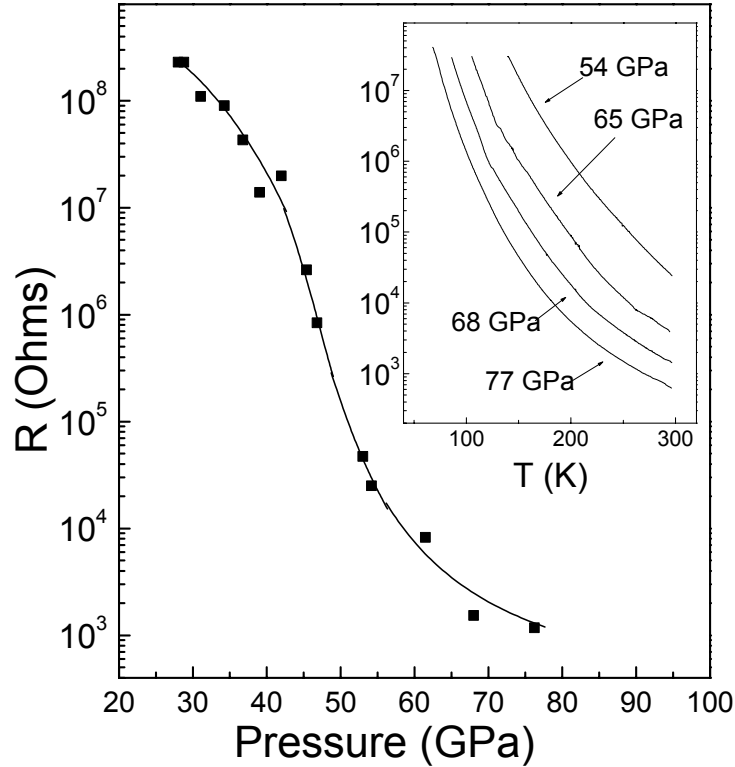


Figure 3. Resistance *versus* pressure in LuFeO₃. In the 27 – 78 GPa range R drops continuously, by more than five-orders of magnitude, 27 GPa was the lowest pressure at which the resistance could be measured.

The intermediate orthoferrites; EuFeO₃, YFeO₃

Mössbauer spectra of EuFeO₃ recorded at 300 K for several pressures and at 54 GPa at several temperatures are shown in Figs. 4a and 4b. As in the case of Lu, the electronic HP phase consists of LS paramagnetic ferric ions and by cooling to $T < T_M$ the ordered magnetically with the same pattern as in Lu, namely through a weak exchange interaction as evident by the Mössbauer relaxation spectra. The experimental spectra at $T < T_M$ were fit with a program adapted from Nowik and Wickman [13] from which $\tau \sim 5 \times 10^{-8}$ s was deduced. The theoretical spectra are depicted as solid lines through the experimental points. The onset of a ${}^2T_{2g}$ LS state is also manifested by the strong T-dependence of the quadrupole splitting clearly observed (see Fig. 4b). Both our preliminary XRD data and the IS (see Fig. 1) suggest a first-order phase transition accompanied by a volume drop. Similar results were obtained for YFeO₃.

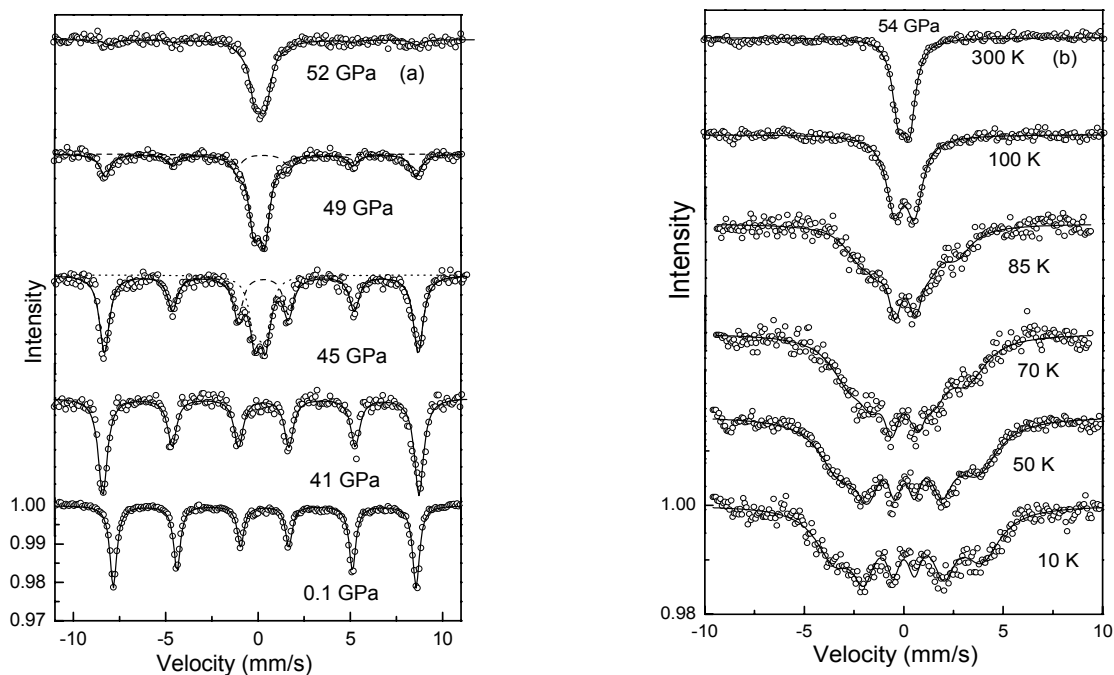


Figure 4. (a) The evolution of the HP phase in EuFeO₃ as observed by MS at RT. The HP phase is paramagnetic and characterized by a single quadrupole-split component with QS considerably smaller than that of YFeO₃. (b) The onset of the magnetic ordering of the LS ferric moments at $T < 90$ K. Note the strong QS-temperature dependence (100 and 300 K). Solid lines are the convoluted theoretical fit to the experimental spectra. The dotted lines correspond to the spectral components.

The largest orthoferrites; PrFeO₃, LaFeO₃

Not like the previous cases the *large R*-orthoferrites undergo first-order transition into two equally abundant magnetic sublattices; composed of high-spin and low-spin Fe³⁺ sites. This is demonstrated in Fig 5a; starting at 40 GPa the new electronically composite phase is observed characterized by two quadrupole-split components with different values of QS and IS. The component with the smaller QS and IS corresponds to the HS sublattice. And indeed, by cooling the sample to 5 K both species become magnetically ordered: the HS-ferric with a typical sextet Zeeman splitting and the LS-ferric with the spin-spin fluctuating spectrum. Pressure increase results in further increase of the crystal-field of the gradual and eventually total collapse of the HS state as seen in Fig. 5b. In the cases of the *large* orthoferrites, pressure increase to beyond 100 GPa results in an insulator-metal transition concurrent with the collapse of the magnetic moment, e.g., the *Mott* transition. This has been extensively reported in Ref. 2.

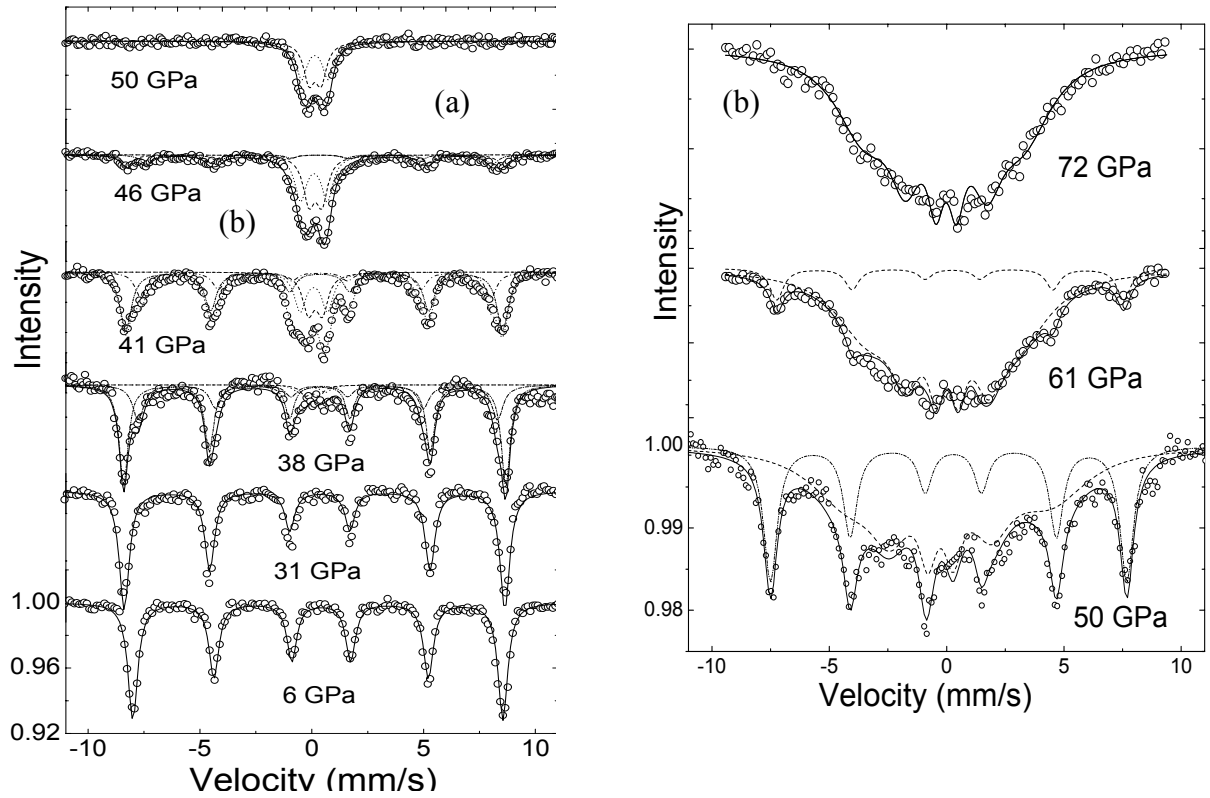


Figure 5. (a) The Mössbauer spectra of PrFeO_3 at ambient temperature as a function of pressure. The HP phase, not like the *intermediate* and *smallt R*-orthoferrites, consists at its formation of two paramagnetic ferric sublattices: a HS (small QS) and LS with rather equal abundance. (b) Upon cooling to 5 K they become magnetically ordered, the HS with its Zeeman-split sextet and the LS component with its spin-spin relaxation sub-spectrum. With further pressure increase one witnesses the gradual HS to LS conversion, reaching 100% at 70 GPa.

The Mott-Hubbard phase diagram of La and Pr orthoferrites

Measurements to ~ 200 GPa both by MS and resistance allowed to derive the *Mott-Hubbard* phase diagram of the La and Pr orthoferrites. The order parameter used was the H_{hf} (Fe) which is proportional to magnetic moment and P which is related to t/U (Ref. 5). The diagram is shown in Fig. 6.

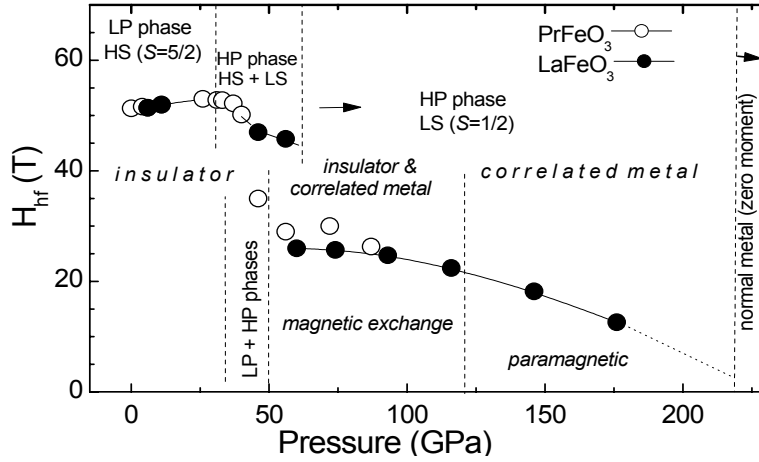


Figure 6. The phase diagram of $R\text{FeO}_3$ in terms of the hyperfine-field as a function of pressure. The solid lines are guides to the eyes, and the vertical dotted lines delineate various ranges in the *Mott-Hubbard* diagram. In the LP phase, up to ~ 35 GPa, H_{hf} increases slightly possibly due to increase in T_N with P . In the 35 – 50 GPa pressure range the HP and the LP phases coexist, and between 50 – 70 GPa the HP phase is composed of both LS and HS states with the abundance of the HS decreasing with pressure. Up to ~ 70 GPa the material is a *bona-fide* insulator ($U/t > 1$). Beginning at 70 GPa, up to 120 GPa, the LS state still shows magnetic exchange with a progressive decrease of H_{hf} (magnetic moment). In this range both the correlated metal and the insulator states coexist with the abundance of the latter decreasing with increasing pressure. The state at $P > 120$ GPa is *paramagnetic*, and the metal is correlated. In LaFeO_3 , based on extrapolation to $H_{\text{hf}} = 0$, a normal metal state ($U/t \ll 1$) is expected to occur at ~ 220 GPa.

DISCUSSION

A substantial increase in the crystal field due to pressure results in a spin-crossover in $R\text{Fe}^{3+}\text{O}_3$. Consequently, a new HP phase is created in which the magnetic ordering temperature T_M is greatly reduced, from 600-700 K to ~ 100 K. The nature of the magnetic ordering of the HP phase is not established. The onset of the LS phase particularly affects the crystallographic states of the *intermediate* and *large* orthoferrites ensuing in a volume reduction of $\sim 4\%$ as observed by XRD and the equation of state (see Fig. 7) and via the jump in the IS (fig. 1). It should be noted that in both La and Pr cases the HP phase is formed in both HS and LS species, not like the intermediate *R*-orthoferrites where the HP phase at its inception is in a pure LS configuration. However the case of LuFeO_3 is strictly different. Preliminary XRD data reveals an **continuous** volume decrease with pressure accompanied by a volume drop ($\sim 4\%$) at P_C yet $\Delta\text{IS}/\text{IS}(P_C) \sim 0$ (see Fig. 1). A plausible explanation based on the IS results is that spin-crossover does not affect considerably the Fe-O octahedral volumes and that the volume change is due to their possible tilting with respect to *c*-axis. Further studies are being carried to elucidate this problem.

The large R -orthoferrites, due to their large R^{3+} ionic radii cannot accommodate even the presence of $\sim 50\%$ of the LS species with its reduced octahedral volume ensuing volume shrinkage.

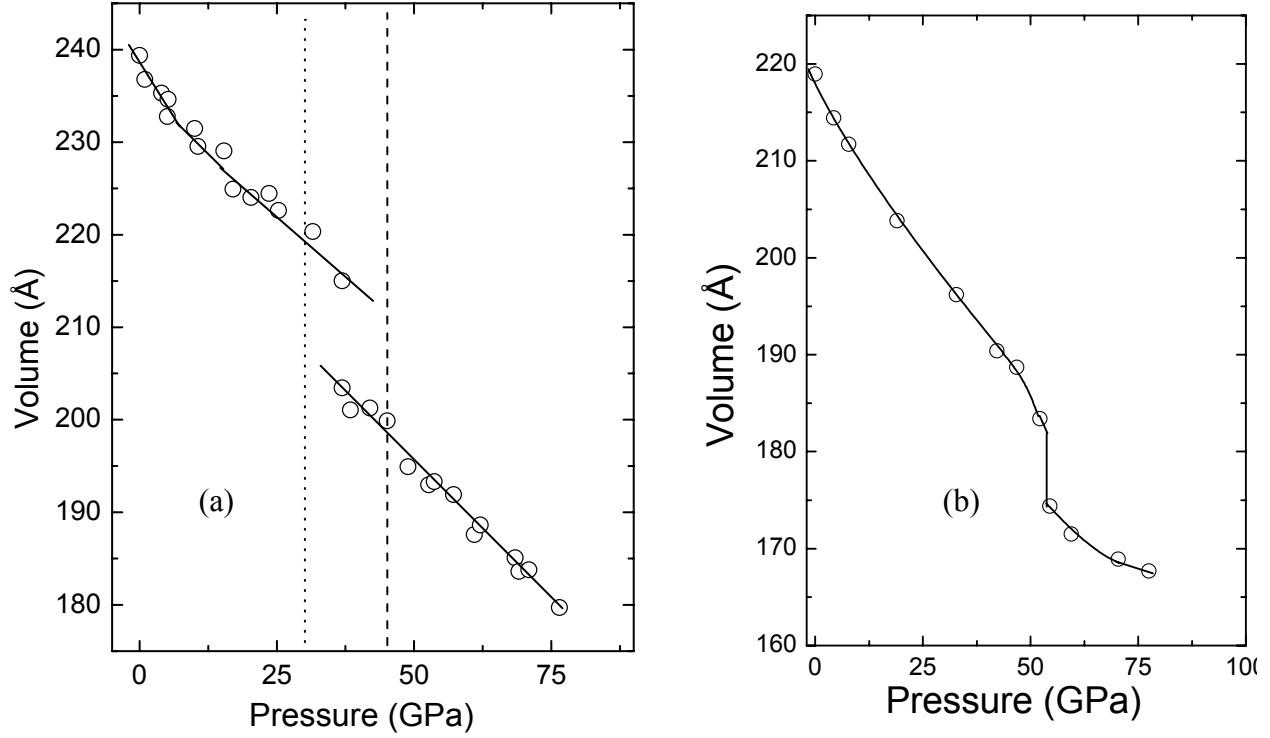


Figure 7 Preliminary results of the equation of states of PrFeO₃ (a) and of LuFeO₃ (b). The lines through the experimental points are for guiding the eyes. In both cases there is a drop in V at $\sim P_C$ but for the Pr-orthoferrite one clearly sees a *coexistence region* in which both the HP and LP phases coexist due to a sluggish transition. The relative changes in volume at the transition are $\sim 6\%$ and 4% for Pr and Lu, respectively. The PrFeO₃ phase transition is accompanied by a new HP phase.

Acknowledgement

This research was supported in parts by BSF Grant 9800003, by Israeli Science Foundation Grant 1998003, and by LANL-UC IGPP program Grant 919R. We thank the personnel of the ID30 beam (ESRF) for their assistance.

References:

- 1 M. Eibschutz, S. Strikman, and D. Treves, *Phys. Rev.* **158**, 562 (1967).
- 2 W.M. Xu, O. Naaman, G.Kh. Rozenberg, M.P. Pasternak, and R.D. Taylor, *Phys. Rev B* **64**, 094411 (2001).
- 3 M. P. Pasternak, G. Kh. Rozenberg, G. Yu. Machavariani, O. Naaman, R. D. Taylor, and R. Jeanloz, *Phys. Rev. Letters.* **82**, 4663 (1999).
- 4 An exceptional case of a temperature-dependent *Mott* transition has been observed in $RNiO_3$ (see J. B. Torrance *et al.*, *Phys. Rev. B* **45**, 8209 (1992)).
- 5 The Hubbard Hamiltonian $H = \sum t_{ij} a_{i\sigma}^+ a_{j\sigma} + U \sum n_i^\uparrow n_i^\downarrow$, is the simplest description of a *Mott-insulator* (J. Hubbard, *Proc. Royal. Soc. A* **277**, 237 (1964)). It is characterized by a kinetic energy term t_{ij} denoting the hopping of an electron from site i to its nearest neighbor site j and by the extra energy cost U of putting two electrons ($n_i^\uparrow n_i^\downarrow$) on the same site. The bandwidth W is proportional to t . In the case of *charge transfer* insulator, U , the energy gap separating the *empty* and *filled d*-bands, is replaced by Δ , a gap between the *empty d*-band and *filled-ligand* bands (J. G. Zaanen, G. A. Sawatzky, and J. W. Allen, *Phys. Rev. Letters* **55**, 418 (1985)). With pressure increase the bandwidth increases allowing the use of P as a measure of t/U .
- 6 S. A. Carter, T. F. Rosenbaum, M. Lu, and H. M. Jaeger, P. Metcalf, J. M. Honig, and J. Spalek, *Phys. Rev. B* **49**, 7898 (1994).
- 7 G.Yu. Machavariani, M P. Pasternak, G.R. Hearne, and G.Kh. Rozenberg, *Rev. Sci. Instr.* **69**, 1423 (1998).
- 8 Due to the proximity of electrodes ($\sim 10 \mu m$), there was no need for a pressure medium.
- 9 A.P. Hammersley, S.O. Svensson, M. Hanfland, A.N. Fitch, and D. Hausermann, *High Pressure Res.* **14**, 235 (1996).
- 10 G.R. Hearne, M. P. Pasternak, and R. D. Taylor, *Rev. Sci. Inst.* **65**, 3787 (1994).
- 11 The IS in ^{57}Fe is proportional to the *negative* value of the *s*-electron density at the nucleus $\rho_s(0)$. **Decrease** in IS is concomitant to the **increase** in $\rho_s(0)$, e.g., in the density at and around the Fe ion.
- 12 D.M. Sherman in *Advances in Physical Geochemistry*, edited by S. K. Saxena, (Springer-Verlag, 1988) V. 7, p. 113.
- 13 I. Nowik and H. H. Wickman, *Phys. Rev. Lett.* **17**, 949 (1966).

Mat. Res. Soc. Symp. Proc., **718**, D2.7.1 (2002).